Journal of the European Ceramic Society 39 (2019) 4144–4148

Contents lists available at ScienceDirect

Journal of the European Ceramic Society

journal homepage: www.elsevier.com/locate/jeurceramsoc

Original Article

Giant suppression of dielectric loss in $BaZrO_3$

T. Kolodiazhnyi[a,*], P. Pulphol[b], W. Vittayakorn[b], N. Vittayakorn[b]

[a] National Institute for Materials Science, 1-1 Namiki, Tsukuba, Ibaraki 305-0044, Japan
[b] Electroceramic Research Laboratory, College of Nanotechnology and Advanced Material Research Unit, Faculty of Science and Nano-KMITL Center of Excellence on Nanoelectronic Devices, King Mongkut's Institute of Technology Ladkrabang, Bangkok 10520, Thailand

ARTICLE INFO

Keywords:
$BaZrO_3$
Dielectric loss
Point defects
Dielectric resonators
Sintering

ABSTRACT

We report the effect of precursor's purity and heterovalent substitution on the microstructure and dielectric properties of $BaZrO_3$ ceramics. We find that independent of the purity or raw materials, the dielectric loss of $BaZrO_3$ at microwave frequencies is rather high with a Q factor in the range of 1000–3000 at 10 GHz. All stoichiometric ceramics studied show up to three types of low-T dielectric relaxations in the 2–250 K range. All these dielectric anomalies can be suppressed by partial substitution of Zr for Nb. By alloying of $BaZrO_3$ with a hypothetical $BaGa_{1/2}Nb_{1/2}O_3$ phase the $Q \times f$ value of ceramics at microwave frequency can be improved significantly. The origin of this remarkable improvement is attributed to the effect of the donor ions on the random electric fields and antiferrodistortive instability. Ceramic with a chemical composition of $BaZr_{0.96}Ga_{0.02}Nb_{0.02}O_3$ sintered at 1600 °C shows dielectric constant, $\varepsilon' = 36.7$, temperature coefficient of the resonance frequency, $\tau_f = +110$ ppm/°C and $Q \times f = 172$ THz.

1. Introduction

$BaZrO_3$ is an important ceramics that is mainly used as a membrane for proton conducting fuel cells [1] and as an additive to microwave dielectric resonators [2]. Despite its simple cubic perovskite structure with Goldschmidt tolerance factor very close to unity (i.e., $t = 1.004$), $BaZrO_3$ continues to challenge the research community. Recent attempts to understand its crystal structure using the density-functional theory (DFT) produced somewhat conflicting results [3–6]. The first-principles calculations mostly predict a non-cubic (i.e., orthorhombic) structure in disagreement with the low-temperature neutron diffraction data which indicates the cubic symmetry (*Pm*3*m* space group) [3]. In contrast to the diffraction data, several experimental findings including Raman, far-infrared, and time-domain terahertz spectroscopies indicate that the local crystal symmetry of $BaZrO_3$ is lower than cubic, although the symmetry distortions are very weak [7–9]. It was suggested in Ref. [3] that, while the antiferrodistortive (AFD) oxygen cage rotations are present on the dynamic scale, their long-range-order condensation at low temperatures is precluded by the zero-point quantum effects or by the point-defect-induced lattice disorder.

According to the DFT calculations of $BaZrO_3$, the phase transition to the low symmetry phase will result in a notable drop in the dielectric constant due to the 40% decrease in the contribution from the low-energy Last phonon mode [4]. Although no clear phase transition was found, two low-T dielectric humps where detected in the $\varepsilon'(T)$ dependence of $BaZrO_3$ in Ref. [3]: one at ~15 K and another at ~50–65 K. The former one was tentatively attributed to the 'activation of the oxygen octahedra rotation' reminiscent to the onset of the low-symmetry phase transition on the local scale, whereas the latter one was assigned to the frequency-dependent dipolar relaxation of extrinsic point defects [3].

The room-temperature microwave dielectric properties of $BaZrO_3$ show surprisingly high dielectric loss, tan δ (tan $\delta = 1/Q$, where Q is the quality factor). The typical values of the $Q \times f$ product (f is a resonance frequency) of the $BaZrO_3$ dielectric resonators at $f \approx 10$ GHz are in the range of 5–20 THz [10–13]. These low values of Q-factor of $BaZrO_3$ are rather unusual, bearing in mind the modest value of the dielectric constant, $\varepsilon' = 36$, the perfect crystal packing, and the ionic character of the Zr-O bond.

In this paper we look for possible sources of the low Q-factor in $BaZrO_3$ including purity of the raw materials, ceramic density, microstructure and point defects. While we cannot see a clear correlation between the purity of the raw powders and the dielectric loss, we find that the microwave dielectric properties at ~10 GHz are closely related to the low-temperature dielectric anomalies detected at radio-frequency range. We find that intentional acceptor impurities are detrimental to the Q-factor at 10 GHz, whereas small concentration of intentional donor impurities significantly reduces the dielectric loss. By proper

* Corresponding author.
E-mail address: kolodiazhnyi.taras@nims.go.jp (T. Kolodiazhnyi).

https://doi.org/10.1016/j.jeurceramsoc.2019.06.037
Received 15 March 2019; Received in revised form 18 June 2019; Accepted 21 June 2019
Available online 22 June 2019
0955-2219/

choice of hetero-valent substitution of Zr host with both donor and acceptor ions, the low-T dielectric relaxations are completely suppressed and the microwave Q-factor of $BaZrO_3$ is dramatically improved from $Q \times f \sim 20$ to 172 THz, thus making it more attractive candidate for practical applications in microwave ceramics.

2. Experimental

To investigate the effect of the precursor's purity on the dielectric properties, the stoichiometric $BaZrO_3$ (BZ) specimens were prepared using precursors of different purity, i.e., $BaCO_3$ (99%, 99.9% and 99.99%) and ZrO_2 (99%, 99.9% and 99.99%). $BaZrO_3$ prepared from precursors of 99%, 99.9% and 99.99% purity are abbreviated as BZ-2N, BZ-3N and BZ-4N, respectively. In addition, to study the effect of donor and acceptor dopants, the BZ-3N samples were substituted at Zr site with Ga and Nb. The Ga_2O_3 (99.9%) and Nb_2O_5 (99.98%) oxides were used as a source of Ga and Nb ions. The starting powders were mixed in plastic bottles with Y-stabilized ZrO_2 balls and ethanol. After drying the homogenized mixtures were heat treated at 1300 °C for 10 h in air to remove CO_2. Sintering of disk-shaped compacts was performed at 1550–1650 °C for 10–20 h. Phase composition was studied by powder X-ray diffraction (Rigaku Miniflex600 X-ray diffractometer with Cu K_α X-ray source). Lattice parameters where obtained from Le Bail refinement of the powder X-ray data (PXRD) using Jana2006 [14]. The relative density was calculated as a ratio of experimental density over the theoretical density determined from the unit cell volume. Dielectric properties in the 10 Hz–500 kHz range were studied in the 2–360 K interval using commercial cryostat (Quantum Design, US) and impedance analyzer (Alpha Novocontrol, Germany). Microwave characterization at ~10 GHz included the measurements of dielectric constant, Q-factor, and temperature coefficient of the resonance frequency, τ_f, according to the method described in Ref. [15]. The τ_f was measured in a temperature range of 22–80 °C.

3. Results and discussion

Powder X-ray diffraction of the BZ-2N, BZ-3N and BZ-4N ceramics sintered at 1650 °C for 20 h revealed a single phase with a cubic perovskite structure ($Pm3m$ space group) and a lattice unit cell of a = 4.1943(2) Å in agreement with previous studies [3]. No traces of the secondary phases were found in the powder X-ray diffraction pattern (not shown).

The effect of the purity of the raw materials on the microstructure of the $BaZrO_3$ ceramics sintered at 1650 °C for 20 h is shown in Fig. 1. The medium purity (i.e., BZ-3N) ceramics shows the smallest average grain size of 1.8(4) μm, whereas the BZ-2N, BZ-4N ceramics have average grain size of 2.5(3) and 3.2(4) μm, respectively. The BZ-3N ceramics shows the highest porosity (i.e., ~10%) among the studied specimens. The relative density, ρ, the grain size and the microwave dielectric properties of BZ-2N, BZ-3N and BZ-4N sintered at 1650 °C for 20 h are summarized in Table 1.

It is interesting to note that despite small grain size and relatively low density of 90%, the BZ-3N ceramics shows the highest $Q \times f$ = 31 THz among the three types of undoped $BaZrO_3$ ceramics (Table 1). Because of the lower density, the dielectric permittivity of the BZ-3N ceramics is ~31.4, which is smaller than ε' = 36.2 and 35.8 of the BZ-2N and BZ-4N, respectively (see Table 1). Surprisingly, the highest-purity BZ-4N ceramics with high density and the largest grains shows the lowest $Q \times f$ of 15 THz. Therefore, from these initial results we could not detect any obvious correlation between the purity and density on one hand and the dielectric properties of $BaZrO_3$ on the other hand.

Table 1
Relative density (ρ), averaged grain size (d) and microwave dielectric properties, such as ε', $Q \times f$ and τ_f at ~10 GHz for $BaZrO_3$ and BZ–BGN ceramics sintered at 1650 °C for 20 h. The $BaZr_{0.99}Ga_{0.01}O_3$ and $BaZr_{0.995}Nb_{0.005}O_3$ ceramics were sintered at 1600 °C for 20 h. The numbers in front of BZ and BGN indicate mole percent.

	ρ (%)	d (μm)	ε'	$Q \times f$ (THz)	τ_f (ppm/°C)
BZ-2N	97.8(9)	2.5(3)	36.2(3)	25(1)	+114(4)
BZ-3N	90(2)	1.8(4)	31.4(3)	31(1)	+118(4)
BZ-4N	96.3(9)	3.2(4)	35.8(3)	15(1)	+121(5)
$BaZr_{0.995}Nb_{0.005}O_3$	96.2(9)	1.3(4)	35.8(3)	77(1)	+119(4)
$BaZr_{0.99}Ga_{0.01}O_3$	97.1(5)	3.7(3)	36.4(3)	8.4(5)	+117(5)
99BZ-1BGN	97.9(5)	3.2(4)	36.3(3)	96(1)	+111(5)
98BZ-2BGN	96.7(5)	3.1(4)	36.2(3)	147(1)	+113(2)
96BZ-4BGN	99.0(5)	3.9(6)	36.7(3)	168(1)	+107(5)
92BZ-8BGN	98.5(5)	3.5(4)	36.6(3)	129(1)	+100(4)
88BZ-12BGN	98.7(5)	1.0(1)	36.7(3)	99(1)	+89(4)
80BZ-20BGN	98.0(5)	1.7(2)	36.9(3)	74(1)	+77(7)

To explicitly estimate the effect of extrinsic impurities on the dielectric properties of $BaZrO_3$, we prepared donor-doped $BaZr_{0.995}Nb_{0.005}O_3$ and acceptor-doped $BaZr_{0.99}Ga_{0.01}O_3$ single-phase ceramics. Their properties are listed in Table 1 and their microstructure is shown in Fig. 2h, i. It is noted that the $Q \times f$ = 77 THz of Nb^{5+}-doped $BaZrO_3$ is almost an order of magnitude higher than that of Ga^{3+}-doped $BaZrO_3$ ($Q \times f$ = 8.4 THz) despite the higher density and larger grains of the latter ceramics (see Fig. 2h, i). We conclude, therefore, that the heterovalent substitution of Zr ions with donors improves the Q-factor of $BaZrO_3$, whereas substitution with acceptors significantly improves the density and the grain morphology but surprisingly decreases the Q-factor.

To combine the benefits of these two effects we explored the $BaZrO_3$ co-doped with both acceptors (Ga) and donors (Nb). For this purpose we prepared several $BaZrO_3$ ceramics alloyed with a hypothetical $BaGa_{1/2}Nb_{1/2}O_3$ phase, abbreviated hereafter as BGN. According to our findings, $BaZrO_3$ forms a solid solution with the hypothetical BGN end member up to at least 20 mol% of BGN. The $(1-x)BaZrO_3$–xBGN solid solution has a cubic symmetry with the unit-cell lattice parameter decreasing linearly with an increase in x (see Fig. 3).

The microstructure of the $(1-x)BaZrO_3$–xBGN ceramics sintered at 1650 °C for 20 h is shown in Fig. 2a–g and the average grain size, relative density and selected dielectric properties are listed in Table 1.

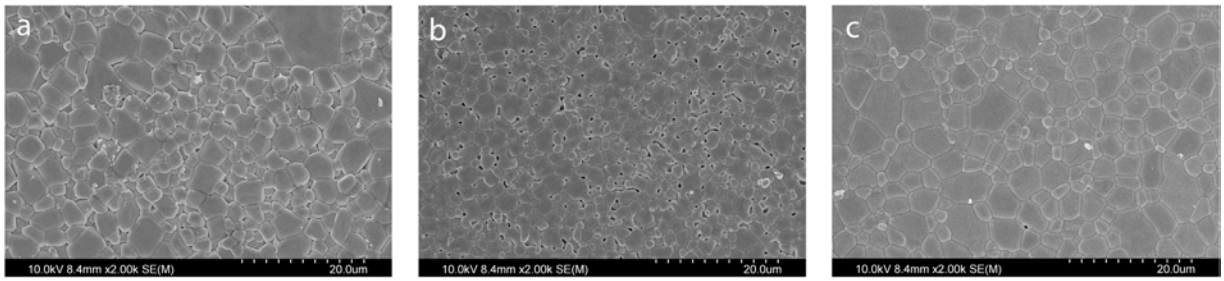

Fig. 1. SEM images of the surface of the BZ-2N (a), BZ-3N (b) and BZ-4N ceramics sintered at 1650 °C for 20 h. The 20 μm scale marker is shown at the bottom right part of the image.

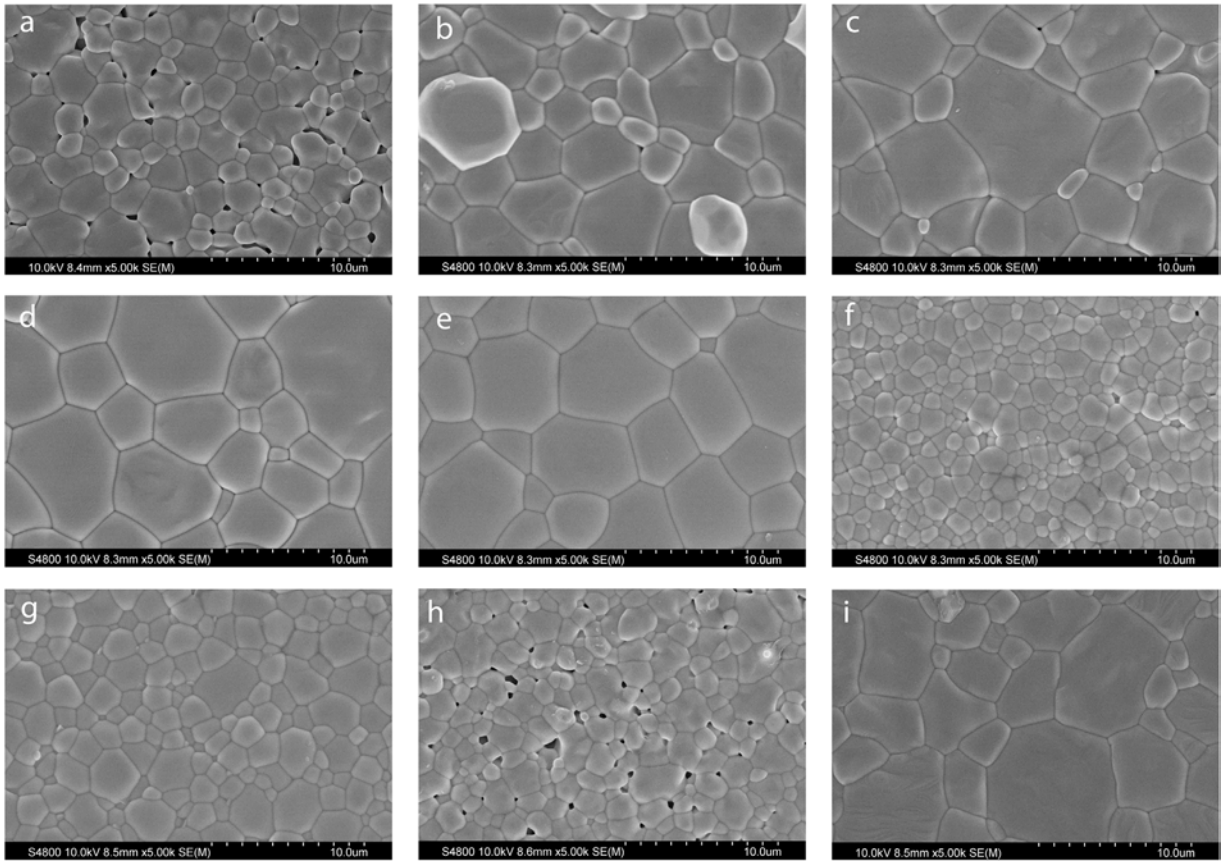

Fig. 2. SEM images of the top surface of the BZ-3N (a), 99BZ-1BGN (b), 98BZ-2BGN (c), 96BZ-4BGN (d), 92BZ-8BGN (e), 88BZ-12BGN (f), 80BZ-20BGN (g) ceramics sintered at 1650 °C for 20 h. The $BaZr_{0.995}Nb_{0.005}O_3$ (h) and $BaZr_{0.99}Ga_{0.01}O_3$ (i) ceramics were sintered at 1600 °C for 20 h. The 10 μm scale marker is shown at the bottom right part of the image.

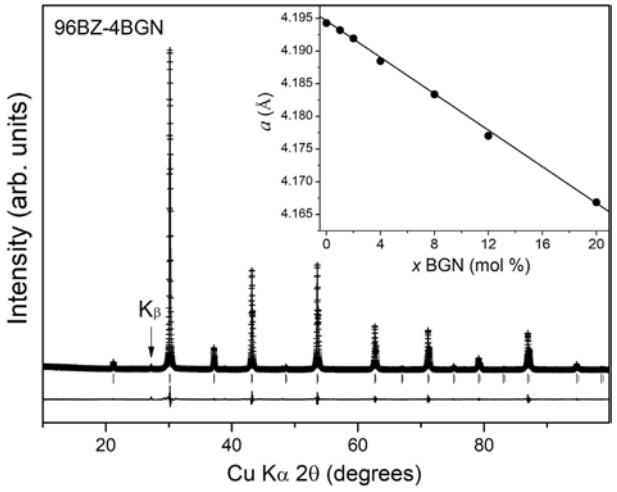

Fig. 3. Room temperature x-ray diffraction pattern (+) of 96BZ-4BGN sintered at 1650 °C for 20 h. Calculated diffraction pattern from Le Bail refinement (*Pm3m* space group) is shown by solid line. The vertical bars indicate the positions of expected Bragg peaks. The difference between observed and calculated data is shown at the bottom of the plot. The inset shows the evolution of the unit cell of BZ-BGN solid solution as a function of mole percent of BGN.

In addition to a significant improvement in the relative density and ε', alloying with BGN also reduces the sintering temperature of $BaZrO_3$ ceramics from 1650 to 1550 °C without sacrificing the dielectric properties (see Fig. 4). Remarkably, the $Q \times f$ product of $(1-x)BaZrO_3$–xBGN ceramics increases significantly with x, goes through a maximum at ~4 mol% of BGN and gradually decreases at higher x. The 96BZ-4BGN ceramics sintered at 1600 °C for 20 h shows a maximum $Q \times f$ of ~172 THz (Fig. 4) One may notice that the average grain size of the BZ-BGN initially increases up to 4 mol% of BGN and then decreases from 3.5 μm to 1.0 μm when the concentration of BGN exceeds 8 mol% (see Fig. 2 and Table 1). While it is possible that a sudden drop in grain size at $x \geq 0.08$ may partially account for a gradual decrease in the Q-factor, more work is needed to clarify this hypothesis.

Based on Shannon's ionic radii data, the effective ionic radius of $r_{Ga_{1/2}Nb_{1/2}} = 0.63$ Å is smaller than that of $r_{Zr^{4+}} = 0.72$ Å [16]. Therefore, the Goldschmidt tolerance factor, t, of the $(1-x)BaZrO_3$–xBGN increases from 1.004 for $x = 0$ to 1.0126 for $x = 0.2$ [17]. According to the hypothesis of Reaney et al. [18], an antiphase oxygen octahedral instability in perovskites occurs at a critical t_c of ~0.99. At $t > t_c$ most perovskites have untilted oxygen octahedra framework. As a result, for $t \geq 0.99$ the temperature coefficient of the resonance frequency gradually decreases from a highly positive to a slightly negative values [18]. It is not surprising, therefore, to see that as the t of the $(1-x)BaZrO_3$–xBGN solid solution increases from 1.004 to 1.0126 with increasing x, the τ_f shows a gradual decrease from $+118 \pm 4$ to $+75 \pm 7$ ppm/°C (Fig. 4d).

It is interesting to compare the microwave Q-factor of $BaZrO_3$ ceramics with intrinsic limit imposed by the lattice anharmonicity. Extrapolation of the infra-red optical conductivity to microwave range to predict the intrinsic limit of microwave dielectric loss is a very common practice that has been successfully applied to many microwave ceramics [19,20]. The intrinsic limit of the microwave dielectric loss, ε'', of $BaZrO_3$ can be estimated by the low-energy extrapolation of the infra-red optical conductivity, $\sigma'(\omega)$, data reported in Ref. [8] according to:

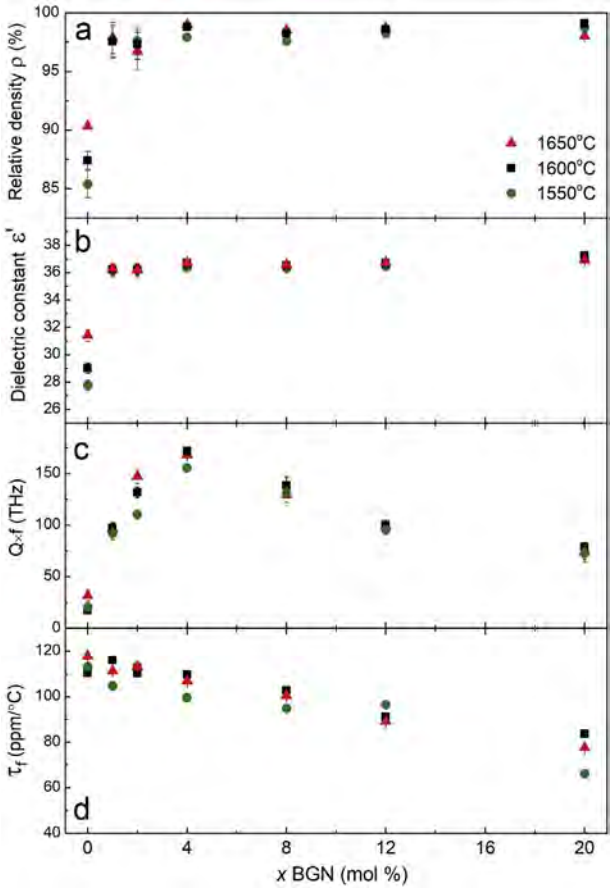

Fig. 4. Relative density (a), dielectric constant (b), $Q \times f$ (c) and τ_f (d) of BZ-BGN ceramics as a function of mole percent of BGN. The legend indicates the sintering temperature at sintering time of 20 h.

$$\varepsilon'' = \frac{\sigma'(\omega)}{\omega\varepsilon_0}, \quad (1)$$

This yields the upper bound limit of the intrinsic $Q \times f$ product of 77 ± 40 THz at a frequency of ~10 GHz. The experimental $Q \times f$ of undoped $BaZrO_3$ ceramics found in this work is in the range of ~15–30 THz which is in agreement with the previous literature data [10–13]. Because the $Q \times f$ = 15–30 THz is much lower than the intrinsic limit of 77 ± 40 THz, it is clear that the microwave dielectric losses in the $BaZrO_3$ ceramics are dominated by the extrinsic factors. This is not an exceptional finding because the $Q \times f$ of vast majority of microwave dielectric resonator ceramics are dominated by the extrinsic loss [21]. What does look unusual in the case of $BaZrO_3$ is that introduction of a large amount of heterovalent point defects and lattice disorder by alloying with BGN causes an enhancement of $Q \times f$ *above the intrinsic limit* of 77 ± 40 THz of pure $BaZrO_3$. Indeed, it appears that a simple cubic perovskite $BaZr_{0.96}Ga_{0.02}Nb_{0.02}O_3$ ceramics shows the highest $Q \times f \approx 172$ THz among the known dielectric resonator materials with $\varepsilon' \geq 36$ (Fig. 4c) [22].

To bring the dielectric loss below the intrinsic limit, alloying with BGN must reduce the damping constant of the $BaZrO_3$ eigenphonons. This interpretation, however, is difficult to comprehend because the lattice disorder in perovskites usually causes an increase in the phonon damping [23]. Another possibility may involve pinning of the local AFD oxygen octahedra rotations by extrinsic defects. If the low-energy excitations associated with the AFD oxygen cage rotations dominate the microwave dielectric loss, an increase in their energy by the random field of heterovalent impurities may indeed suppress the tan δ at microwave frequencies. To explore this hypothesis in detail we studied the temperature dependence of the dielectric properties at lower frequency down to T = 2 K.

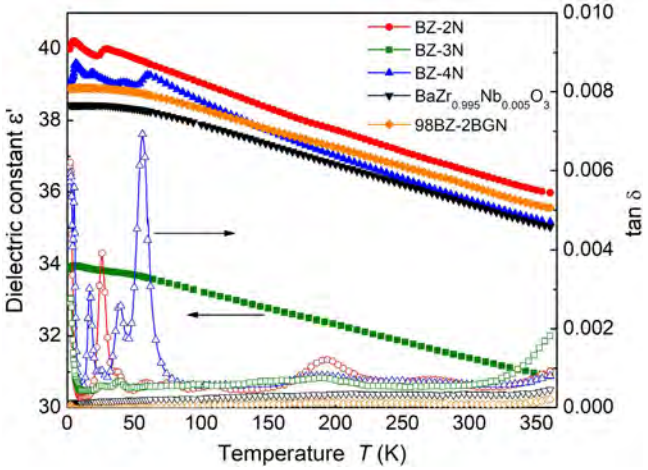

Fig. 5. Dielectric constant, ε', (filled symbols) and loss tan δ (open symbols) at 500 kHz of $BaZrO_3$ ceramics. BZ-3N shows much lower value of the ε' due to the lower density (~90%).

Fig. 5 shows T-dependence of the ε' and tan δ measured at 500 kHz for several $BaZrO_3$ ceramics sintered at 1650 °C for 20 h except for the $BaZr_{0.995}Nb_{0.005}O_3$ which was sintered at 1600 °C for 20 h. In agreement with earlier studies, as temperature decreases, paraelectric $BaZrO_3$ shows gradually increasing ε' from $\varepsilon' \sim 36$ at T = 360 K to $\varepsilon' \sim 40$ at T = 2 K. This behavior is attributed to the softening of the Last phonon mode at ~3.7 THz [8,9]. On top of the (intrinsic) quantum paraelectric dependence of ε' (T), several discernable humps can be found below 100 K in most of the $BaZrO_3$ ceramics (Fig. 5). The ε' (T) anomalies closely correlate with the pronounced peaks in the tan δ (T) data (Fig. 5). These dielectric anomalies can be separated into three families:

(i) A weak hump in ε' at ~5–7 K and a pronounced upturn in tan δ below 11 K is probably attributed to the onset of the local oxygen octahedra rotations as proposed in Ref. [3]. Indeed this anomaly is probably intrinsic in origin as it is almost independent on the purity of the samples studied here and can be detected in all the BZ-2N, BZ-3N and BZ-4N ceramics (Fig. 5).

(ii) A series of tan δ peaks and ε' humps at 11 K < T < 80 K have been previously assigned to the dielectric relaxation due to the extrinsic impurities in $BaZrO_3$ [3]. While this is a very plausible explanation which has a number of literature examples (e.g., Mg:$BaMg_{1/3}Ta_{2/3}O_3$ [15], Mn:$SrTiO_3$ [24], Li:$KTaO_3$ [25], etc.), we find it surprising that there is no clear correlation between the purity of our samples and the magnitude of the tan δ peaks. For example, the highest purity $BaZrO_3$ (99.99%) shows multiple tan δ peaks at 11 K < T < 80 K which are also the strongest among the studied $BaZrO_3$ samples (Fig. 5). Intuitively, if the ε' and tan δ anomalies originate from the extrinsic impurities we would expect that their magnitude will decrease with increasing the purity of the precursors, which is in not supported by our experimental findings. The localized hopping of the bound small polarons may contribute to dielectric loss in perovskites in a wide temperature range [26,27]. For example, in Ref. [26], the low-T dielectric relaxation in n-type $BaTiO_3$ due to Ti^{3+} d-electron hopping bound to La^{3+} and Gd^{3+} donor impurity has been revealed. While we cannot rule out similar relaxation in $BaZrO_3$, we doubt the existence of the Zr^{3+} small polarons due to reduction of Zr^{4+} because of the very stable nature of the Zr^{4+} ions. For example, in $EuZrO_3$ perovskite prepared in highly reducing (hydrogen) atmosphere [28], Zr ion maintains oxidation state of 4+.

(iii) A broad tan δ peak at T ~ 160–210 K in some of our $BaZrO_3$

samples (see BZ-2N in Fig. 5) is attributed to the relaxation dynamics of proton interstitials and will be addressed in a much more detail in a separate publication.

To further investigate the possible origin of the low-T dielectric relaxation anomalies in $BaZrO_3$ we have studied several doped systems. Interestingly, all tan δ peaks are eliminated by substitution of Zr^{4+} host ion with as little as 0.5% of Nb^{5+} (see $BaZr_{0.995}Nb_{0.005}O_3$ data in Fig. 5). This result can be rationalized as a freezing of the dipolar relaxation of extrinsic defects caused by the random-field electrostatic interactions with Nb^{5+} ions. Indeed it is well known that the positional degeneracy of the off-centered point defect impurities is lifted by the local strain as well as by random or external electric fields [29].

Surprisingly, we find that the lowest temperature dielectric anomaly at $T \leq 7$ K is also completely suppressed in the Nb-doped $BaZrO_3$. If the low-T dielectric anomaly is related to the freezing of the local oxygen octahedra rotations in $BaZrO_3$, it is not clear why small concentration of Nb impurities can prevent this freezing process. We also find that similar suppression of the low-T dielectric anomalies is achieved by the BZ-BGN alloying: An example of the ε' and tan δ data for 98BZ-2BGN is shown in Fig. 5. On the other hand, doping with small amounts of acceptors, such as Ga or Y ions, does not suppress the low-T dielectric anomaly (not shown) and does not improve the Q-factor in the microwave range. Therefore, we conclude that the effective charge of the extrinsic defects plays an important role in the low-T dielectric relaxation processes in $BaZrO_3$. Clearly, no traces of the low-T dielectric relaxation can be found in the high-Q BZ-BGN ceramics, whereas, without exception, all the samples with the low-T dielectric anomalies inevitably show low Q-factors at microwave frequencies.

4. Conclusions

In conclusion, undoped stoichiometric $BaZrO_3$ ceramics show rather high dielectric loss with $Q \leq 3000$ at 10 GHz. A partial substitution of Zr^{4+} with Nb^{5+} donor ion improves the Q factor considerably whereas substitution with Ga^{3+} acceptors improves the density and grain size but decreases the Q-factor. Three types of the low-temperature dielectric relaxations in $BaZrO_3$ ceramics where detected and discussed. All these relaxations can be completely suppressed by partial substitution of Zr^{4+} with a small amount of Nb^{5+}. Alloying $BaZrO_3$ with hypothetical $BaGa_{1/2}Nb_{1/2}O_3$ phase brings about dramatic decrease in the microwave dielectric loss with the $Q \times f$ value reaching record-high 172 THz for $BaZr_{0.96}Ga_{0.02}Nb_{0.02}O_3$ ceramics. A unique combination of high Q, moderate ε' and a large positive τ_f makes $BaZrO_3$ an excellent choice for design of temperature compensated composite microwave dielectric resonators.

Acknowledgments

T.K. was supported by internal NIMS projects PA5160 and PA4020. P.P. was supported by KMITL PhD scholarship. The work of N.V. was funded by KMITL under grant 2562-01-05-46. N.V. and T.K. acknowledge the KMITL “Academic Melting-Pot” program KREF206203.

References

[1] Y. Yamazaki, F. Blanc, Y. Okuyama, L. Buannic, J.C. Lucio-Vega, C.P. Grey, S.M. Haile, Proton trapping in yttrium-doped barium zirconate, Nat. Mater. 12 (2013) 647–651.
[2] H. Tamura, T. Konoike, Y. Sakabe, K. Wakino, Improved high-Q dielectric resonator with complex perovskite structure, J. Am. Ceram. Soc. 67 (1984) C-59–C-61.
[3] A.R. Akbarzadeh, I. Kornev, C. Malibert, L. Bellaiche, J.M. Kiat, Combined theoretical and experimental study of the low-temperature properties of $BaZrO_3$, Phys. Rev. B 72 (2005) 205104.
[4] J.W. Bennett, I. Grinberg, A.M. Rappe, Effect of symmetry lowering on the dielectric response of $BaZrO_3$, Phys. Rev. B 73 (2005) 205104.
[5] A. Bilic, J.D. Gale, Ground state structure of $BaZrO_3$: a comparative first-principles study, Phys. Rev. B 79 (2009) 174107.
[6] L. Louis, S.M. Nakhmanson, Structural, vibrational, and dielectric properties of Ruddlesden-Popper Ba_2ZrO_4 from first principles, Phys. Rev. B 91 (2015) 134103.
[7] F. Giannici, M. Shirpour, A. Longo, A. Martorana, R. Merkle, J. Maier, Long-range and short-range structure of proton-conducting Y:$BaZrO_3$, Chem. Mater. 23 (2011) 2994–3002.
[8] D. Nuzhnyy, J. Petzelt, M. Savinov, T. Ostapchuk, V. Bovtun, M. Kempa, J. Hlinka, V. Buscaglia, M.T. Buscaglia, P. Nanni, Broadband dielectric response of Ba(Zr,Ti)O_3 ceramics: from incipient via relaxor and diffuse up to classical ferroelectric behavior, Phys. Rev. B 86 (2012) 014106.
[9] M.A. Helal, T. Mori, S. Kojima, Softening of infrared-active mode of perovskite $BaZrO_3$ proved by terahertz time-domain spectroscopy, Appl. Phys. Lett. 106 (2015) 182904.
[10] H. Stetson, B. Schwartz, Dielectric properties of zirconates, J. Am. Ceram. Soc. 44 (1961) 420–421.
[11] T. Yamaguchi, Y. Komatsu, T. Otobe, Y. Murakami, Newly developed ternary (Ca, Sr, Ba) zirconate ceramic system for microwave resonators, Ferroelectrics 27 (1980) 273.
[12] V. Sivasubramanian, V.R.K. Murthy, B. Viswanathan, Microwave dielectric properties of certain simple alkaline earth perovskite compounds as a function of tolerance factor, Jpn. J. Appl. Phys. 36 (1997) 194–197.
[13] I. Levin, T.G. Amos, S.M. Bell, L. Farber, T.A. Vanderah, R.S. Roth, B.H. Toby, Phase equilibria, crystal structures, and dielectric anomaly in the $BaZrO_3$-$CaZrO_3$ system, J. Sol. State Chem. 175 (2003) 170–181.
[14] V. Petricek, M. Dusek, L. Palatinus, Crystallographic computing system JANA2006: general features, Z. Kristallogr. 229 (2014) 345-L 352.
[15] T. Kolodiazhnyi, Origin of extrinsic dielectric loss in 1:2 ordered, single-phase $BaMg_{1/3}Ta_{2/3}O_3$, J. Eur. Ceram. Soc. 34 (2014) 1741–1753.
[16] R.D. Shannon, Revised effective ionic radii and systematic studies of interatomic distances in halides and chalcogenides, Acta Crystallogr. Sect. A 32 (1976) 751–767.
[17] H.D. Megaw, Crystal structure of double oxides of the perovskite type, Proc. Phys. Soc. 58 (1946) 133–152.
[18] I.M. Reaney, E.L. Colla, N. Setter, Dielectric and structural characteristics of Ba- and Sr-based complex perovskites as a function of tolerance factor, Jpn. J. Appl. Phys. 33 (1994) 3984–3990.
[19] S. Kamba, et al., Relationship between microwave and lattice vibration properties in $BaZn_{1/3}Nb_{2/3}O_3$-based microwave dielectric ceramics, J. Phys. D: Appl. Phys. 37 (2004) 1980–1986.
[20] V.M. Ferreira, J.L. Baptista, S. Kamba, J. Petzelt, dielectric spectroscopy of $MgTiO_3$-based ceramics in the 10^9–10^{14} Hz region, J. Mater. Sci. 28 (1993) 5894–5900.
[21] J. Petzelt, N. Setter, Far infrared spectroscopy and origin of microwave losses in low-loss ceramics, Ferroelectrics 150 (1993) 89–102.
[22] M. Sebastian (Ed.), Dielectric: Materials for Wireless Communication, Elsevier, Amsterdam, The Netherlands, 2008.
[23] T. Kolodiazhnyi, J. Padchasri, R. Yimnirun, Effect of temperature and stoichiometry on the long-range 1:2 cation order in $BaZn_{1/3}Ta_{2/3}O_3$, J. Eur. Ceram. Soc. 38 (2018) 1517–1523.
[24] A. Tkach, P.M. Vilarinho, A.L. Kholkin, Dependence of dielectric properties of manganese-doped strontium titanate ceramics on sintering atmosphere, Acta Mater. 54 (2006) 5385–5391.
[25] U.T. Höchli, M. Maglione, Dielectric relaxation spectroscopy and the ground state of $K_{1-x}Li_xTaO_3$, J. Phys.: Condens. Matter 1 (1989) 2241–2256.
[26] E. Iguchi, N. Kubota, T. Nakamori, N. Yamamoto, K.J. Lee, Polaronic conduction in n-type $BaTiO_3$ doped with La_2O_3 or Gd_2O_3, Phys. Rev. B 43 (1991) 8646–8649.
[27] O. Bidault, M. Maglione, M. Actis, M. Kchikech, B. Salce, Polaronic relaxation in perovskites, Phys. Rev. B 52 (1995) 4191–4197.
[28] T. Kolodiazhnyi, M. Valant, J.R. Williams, M. Bugnet, G.A. Botton, N. Ohashi, Y. Sakka, Evidence of Eu^{2+} electrons in the valence band spectra of $EuTiO_3$ and $EuZrO_3$, J. Appl. Phys. 112 (2012) 083719.
[29] V. Narayanamurti, R.O. Pohl, Tunneling states of defects in solids, Rev. Mod. Phys. 42 (1970) 201–235.